

First Resolved Images of the Mira AB Symbiotic Binary at Centimeter Wavelengths

Lynn D. Matthews¹ and Margarita Karovska¹

ABSTRACT

We report the first spatially resolved radio continuum measurements of the Mira AB symbiotic binary system, based on observations obtained with the Very Large Array (VLA). This is the first time that a symbiotic binary has been resolved unambiguously at centimeter wavelengths. We describe the results of VLA monitoring of both stars over a ten month period, together with constraints on their individual spectral energy distributions, variability, and radio emission mechanisms. The emission from Mira A is consistent with originating from a radio photosphere, while the emission from Mira B appears best explained as free-free emission from an ionized circumstellar region $\sim(1-10)\times 10^{13}$ cm in radius.

Subject headings: binaries: symbiotic – stars: AGB and post-AGB – stars: Individual (Mira AB) — stars: winds, outflows – radio continuum: stars

1. Introduction

Symbiotics are interacting binary systems in which a cool, evolved giant transfers material onto a hotter, compact companion through a stellar wind (e.g., Whitelock 1987). This symbiosis affects the late-stage evolution of both stars and their surrounding medium and may play an important role in shaping the formation of planetary nebulae and in the triggering of Type Ia supernovae (e.g., Munari & Renzini 1992; Corradi et al. 2000). Mira AB is the nearest example of a weakly symbiotic binary. It comprises a pulsating asymptotic giant branch (AGB) star (Mira A=*o* Ceti, the prototype of Mira variables) and a low-mass, accreting companion (Mira B, possibly a white dwarf). The pair has a projected separation of $\sim 0''.5$ (~ 65 AU; Karovska et al. 1997)¹, making this one of the very few wind-accreting binaries in which the components can be spatially and spectrally resolved with current telescopes.

¹Harvard-Smithsonian Center for Astrophysics, 60 Garden Street, Cambridge, MA, USA 02138

¹All physical quantities quoted in the this paper have been scaled to the *Hipparcos* distance of 128 pc.

This system therefore provides a rare opportunity to study the individual components of an interacting binary.

Multiwavelength observations of Mira AB have revealed a complex interacting system with tremendous temporal changes in the components and the circumbinary environment (e.g., Karovska et al. 1997,2001,2005; Wood & Karovska 2004 and references therein). Much of this activity is driven by mass-loss from Mira A ($\dot{M} \approx 2.8 \times 10^{-7} M_{\odot} \text{ yr}^{-1}$) through a cool, low-velocity wind ($V_{\infty} \approx 5 \text{ km s}^{-1}$; Bowers & Knapp 1988). Material from the wind is accreted onto Mira B, forming a hot accretion disk, as evidenced by the presence of numerous rotationally broadened, ultraviolet (UV) emission lines (Reimers & Cassatella 1985).

Chandra observations carried out in 2003 December detected an unprecedented X-ray outburst from Mira A (Karovska et al. 2005). This was followed by an increase in UV emission and H α flaring lasting for about one month. This outburst is very unusual, since the X-rays seem to be originating from the AGB star rather than from the accretion disk of Mira B. The outburst may be associated with a magnetic flare followed by a mass ejection event. To constrain the origin of the outburst and monitor its time evolution, we subsequently began multiwavelength monitoring of the Mira AB system, including radio continuum measurements with the Very Large Array (VLA)².

2. Observations

We observed Mira AB with the VLA during ten epochs between 2004 October 19 and 2005 July 4 (Table 1). Data were obtained in 4-IF continuum mode at four frequencies (8.5, 14.9, 22.5, and 43.3 GHz), each with a 100 MHz total bandwidth. Four different array configurations were used (A, BnA, B, and CnB), providing maximum baselines of 36 km, 22 km, 11 km, and 6.5 km, respectively. In some cases, the angular resolution was insufficient to fully resolve Mira AB (see Table 1). Our initial goal at the VLA had been monitoring Mira A at 8.5 GHz; however, upon the detection of radio emission from Mira B, we began obtaining data at additional frequencies in order to constrain the spectral energy distributions of the two sources. Mira A was detected at all four observed frequencies, while Mira B was detected in all but the 14.9 GHz observations.

The data were calibrated and reduced using standard techniques within the Astronomical Image Processing System (AIPS). Absolute flux levels were established through observa-

²The Very Large Array of the National Radio Astronomy Observatory is a facility of the National Science Foundation, operated under cooperative agreement by Associated Universities, Inc.

tions and source models of 3C48 (see Table 1). Interferometric amplitudes and phases were calibrated by using fast switching between Mira and the neighboring point source, 0215-023. A cycle time of 120 s was used to “stop” any rapid tropospheric phase fluctuations, as emission in the Mira field was not strong enough to permit self-calibration. Flux densities for 0215-023 derived from each of our observations are summarized in Table 1. The radio images presented in this paper were computed with the standard CLEAN deconvolution algorithm within AIPS, using a robustness factor $\mathcal{R} = +1$ (Briggs 1995) to weight the visibilities.

3. Analysis and Discussion

Figure 1 shows several examples of our recently obtained radio continuum images of Mira AB. Two continuum sources are clearly detected in each image. After accounting for proper motion, the two sources correspond with the positions of Mira A and B, respectively, as recently determined from *HST* UV observations (Figure 2). This is the first time the components of a symbiotic binary have been resolved unambiguously at centimeter wavelengths.

For each observation, we measured the flux densities of the two stellar components by fitting elliptical Gaussians to the data in the image plane. Our results are summarized in Table 1. Figure 3 plots the derived flux densities of Mira A and B as a function of time.

With one exception, we found Mira A to be brighter than Mira B at all times and at all frequencies. However, our 8.5 GHz measurements on JD 2,453,394 seem to indicate a simultaneous brightening of Mira B and dimming of Mira A compared with our previous measurements, while nine days later, the flux densities of the two are nearly identical. We believe these apparent synchronous variations to be an artifact of undersampling the u - v plane, and were able to reproduce an analogous “redistribution” in flux using pairs of similarly separated artificial point sources introduced into the visibility data. Note however that total flux density (A+B) was conserved. The observations in question were obtained using the BnA configuration of the VLA, which produced a highly elongated beam pattern, with the point spread functions for Mira A & B partially overlapping at 8.5 GHz.

Our observations spanned $\sim 78\%$ of the 332 day pulsation period of Mira A, during which the optical brightness of the star varies by ~ 6 -7 magnitudes (e.g., Reid & Goldston 2002). Our measurements imply that any changes in the radio brightness of either star linked to these pulsations have a substantially smaller amplitude. At 8.5 GHz, where we have the longest observational baseline, the data are consistent with brightness changes of $\lesssim 30\%$ from the mean for both Mira A & B during the 189-day interval between 2004 October 19 and 2005 April 26 ($\lesssim 15\%$ for Mira A excluding the BnA array data; see above).

We have used a weighted mean of the measurements at each frequency where the components of Mira AB were resolved to estimate the spectral indices of the two stars. Figure 4 shows the resulting radio frequency spectra. Both Mira A and B have positive spectral indices, α (where flux density $S_\nu \propto \nu^\alpha$), indicating that the emission mechanism for both sources is likely to be predominantly thermal. Nonlinear least-squares fits to the data show the radio spectra of Mira A and B can be described as $S_{\nu,A} = (0.009 \pm 0.004)\nu_{\text{GHz}}^{1.50 \pm 0.12}$ mJy and $S_{\nu,B} = (0.010 \pm 0.008)\nu_{\text{GHz}}^{1.18 \pm 0.28}$ mJy, respectively.

The initial goal of our radio observations of Mira AB was to search for radio signatures of the recent X-ray outburst detected by Karovska et al. (2005). From the continuum observations obtained to date, we have not detected any unambiguous aftereffects of this event. Some of our radio images of Mira A (e.g., Figure 1) show elongations along a position angle of $\sim 120^\circ$, analogous to those seen in X-rays and in the UV (Karovska et al. 2005). These features could be consistent with an outflow; however, given the phase noise and limited u - v sampling of our data (observations $\lesssim 1$ hour), they may also be spurious. If the X-ray outburst of Mira A was connected with a mass ejection event and/or shock formation, we might also expect a brightening in one or both components of Mira AB. We detected some signs of statistically significant flux density fluctuations in Mira A and in the total flux from the binary at 8.5, 22.5, and 43.3 GHz; however, these are generally limited to a single frequency on a given date, and cannot be unambiguously linked with the outburst. Future monitoring should reveal whether similar-scale fluctuations are the norm for the system. We note that material ejected from Mira A at speeds of ~ 200 km s $^{-1}$ (see Karovska et al. 2005) would require $\gtrsim 1.5$ years to reach the accretion disk of Mira B. Therefore radio signatures of such an event may still occur during late 2005 or 2006.

To gauge the longer-term variability of the Mira AB system, we have also analyzed unpublished archival 8.5 GHz data taken in 1996 December using the VLA in its A configuration. Both Mira A and Mira B were detected with flux densities $S_A = 0.28 \pm 0.05$ mJy and $S_B = 0.15 \pm 0.04$ mJy, respectively. These values are consistent with our recent measurements, and imply changes in the mean brightness of $\lesssim 30\%$ for Mira A and $\lesssim 20\%$ for Mira B during the past 8.5 years.

Previous VLA 8.4 GHz measurements of Mira A have been published by Reid & Menten (1997), based on data obtained during 1990. However, Mira A & B were spatially unresolved in these observations, thus the authors likely measured the *combined* emission from the two binary components. Indeed, their published flux densities agree with the values we derive from the sum of Mira A+B. Reid & Menten (1997) interpreted the radio emission they observed from Mira and other long period variable stars as arising from radio photospheres located at $R \approx 2R_\star$. Their models predict that at centimeter wavelengths (~ 8 -22 GHz) this

emission should exhibit a spectral index $\alpha \approx 1.86$. This is slightly steeper than the value we derive for Mira A (Figure 4). However, after accounting for calibration uncertainties, it is consistent with our data in the range 8.5-22.5 GHz. At higher frequencies, a gradual turnover may be expected owing to opacity changes, consistent with our 43.3 GHz measurements. The Reid & Menten model also predicts an absolute 8.5 GHz flux density for Mira A in agreement with our mean observed value. Our new unblended radio continuum measurements of Mira A therefore remain consistent with the emission arising primarily from a radio photosphere. The limits on brightness fluctuations of $\lesssim 30\%$ over the course of several months furthermore place a limit on shocks or other disturbances in the radio photosphere of Mira A (e.g., resulting from pulsations or the X-ray outburst event) to speeds of less than a few km s^{-1} (see Reid & Menten 1997).

In the case of Mira B, thermal emission from the stellar photosphere and/or accreting surface will be undetectable at centimeter wavelengths owing to the small emitting area. However, Lyman continuum photons from its hot accretion disk or boundary layer may ionize a portion of Mira A’s wind, providing a source of free-free emission. In general, free-free radiation from a fully ionized stellar wind results in radio emission with a spectral index $\alpha = 0.6$ (Wright & Barlow 1975). Our measured spectral index for Mira B is a factor of two steeper than this, and is also steeper than values previously measured for other (unresolved) symbiotics over this frequency range (Seaquist & Taylor 1990). However, in the limit where only a very small fraction of the wind is ionized, the model of Seaquist et al. (1984) and Taylor & Seaquist (1984) (the so-called “STB” model) predicts $\alpha \rightarrow 1.3-2.0$ across the optically thick portion of the spectrum, consistent with our measurements. Assuming a canonical electron temperature of $T_e = 10^4$ K (Osterbrock 1989), the radius of an optically thick ionized sphere required to produce the observed $\nu=8.5$ GHz emission from Mira B can be estimated as $R = [S_\nu c^2 d^2 / 2kT_e \nu^2 \pi]^{0.5} \approx 1.6 \times 10^{13}$ cm (~ 1 AU) where c is the speed of light and k is Boltzmann’s constant. This suggests an ionized volume much smaller than the binary separation.

An alternate constraint on the size of an ionized region surrounding Mira B may be obtained by incorporating results from previous studies. Based on UV spectroscopy, Reimers & Cassatella (1985) estimated a radius and thickness for the Mira B accretion disk of $r \sim 1.7 \times 10^{11}$ cm and $t \sim 6.8 \times 10^9$ cm, respectively, and an electron temperature $T_e = 11,000$ K. A blackbody with this emitting area and temperature will produce $N_{\text{UV}} \approx 5 \times 10^{41}$ hydrogen-ionizing photons per second. Assuming a separation between Mira A & B of $a=100$ AU (slightly larger than the projected separation), we can also estimate the particle density from the wind of Mira A at the location of Mira B as $n_e = \dot{M} / 4\pi \mu m_H V_\infty a^2$ (Wright & Barlow 1975, Eq. 2), where \dot{M} and V_∞ are Mira A’s wind parameters, μ is the mean molecular weight (~ 1), and m_H is the mass of a hydrogen atom. This predicts $n_e \approx 7.2 \times 10^5 \text{ cm}^{-3}$,

neglecting density enhancements caused by the gravitational field of Mira B. In the idealized case of a pure hydrogen medium of uniform density, the size of the resulting ionized region as predicted by the Strömngren relation (e.g., Osterbrock 1989) is $R_s \approx (3N_{\text{UV}}/4\pi\alpha_r n_e^2)^{\frac{1}{3}} \approx 9.8 \times 10^{13}$ cm. Here α_r is the recombination coefficient to all levels but the ground state of hydrogen ($\approx 2.6 \times 10^{-13}$ cm³ s⁻¹; Osterbrock 1989). Although this order-of-magnitude estimate neglects such factors as a non-uniform density within the ionized volume and the presence of molecules and heavier elements in the wind, it supports the STB model as an explanation for the radio emission from Mira B and reaffirms that any ionized nebula around the star should be quite small compared with the binary separation and the overall extent of Mira A’s circumstellar envelope ($> 10^{17}$ cm; Bowers & Knapp 1988). It is also consistent with the nebula being unresolved by our recent VLA observations (predicted angular diameter $\theta \lesssim 0''.1$). Future VLA measurements should provide additional constraints on the size and shape of this ionized region, and ultimately place new, independent constraints on the Mira B accretion disk properties and the true binary separation.

We have considered other possible mechanisms as the source of the radio emission from Mira B, but none appear likely to contribute appreciably to the observed flux. For example, if Mira B is a magnetically active dwarf rather than a white dwarf (Jura & Helfand 1984; Kastner & Soker 2004), its quiescent radio luminosity is expected to be $\sim 10^{12}$ - 10^{14} erg s⁻¹ Hz⁻¹ (Benz & Güdel 1994)—undetectable at Mira B’s distance. Mira B is also known to power a variable wind (Wood et al. 2002), but even if fully ionized, it is too feeble to produce detectable radio emission. Based on the parameters derived by Wood et al. (2002): $\dot{M} \approx (0.14\text{-}2.8) \times 10^{-11} M_{\odot} \text{ yr}^{-1}$ and $V_{\infty} = 250\text{-}400$ km s⁻¹, the predicted radio flux density from Mira B’s wind (see Wright & Barlow 1975, Eq. 8) would be ~ 4 orders of magnitude smaller than the observed emission. Finally, the steep spectral index of the radio emission from Mira B ($\alpha > 0.6$) and low energy flux of its wind argue against any significant contribution from non-thermal emission produced by collisions between the two winds of the binary (see Dougherty & Williams 2000; Kenny & Taylor 2005).

In summary, we have presented new centimeter wavelength images of the symbiotic binary system, Mira AB. These data allow for the first time measurements of the radio properties of the individual components of a symbiotic binary. Over the frequency range 8-43 GHz, the radio properties of the evolved giant, Mira A, are consistent with the radio emission originating predominantly from a radio photosphere. The emission from Mira B is consistent with arising from a circumstellar H II region $\sim (1\text{-}10) \times 10^{13}$ cm in radius. We find the radio variability of both stars to be $\lesssim 30\%$ over a ten month period during 2004-2005. Flux densities we derived from archival data taken in 1996 are consistent with our recent measurements, and imply changes in the mean 8.5 GHz flux densities of $\lesssim 30\%$ for Mira A and $\lesssim 20\%$ for Mira B during the past 8.5 years.

We thank M. Reid for valuable discussions, and are grateful to the VLA staff for their support of this project. LDM was funded by a Clay Fellowship from the Smithsonian Astrophysical Observatory (SAO). MK is a member of the *Chandra* X-ray Center, which is operated by SAO under contract to NASA NAS8-39073.

REFERENCES

- Benz, A. O. & Güdel, M. 1994, *A&A*, 285, 621
- Bowers, P. F. & Knapp, G. R. 1988, *ApJ*, 332, 299
- Briggs, D. S. 1995, PhD thesis, New Mexico Institute of Mining and Technology
- Corradi, R. L. M., Livio, M., Schwarz, H. E., & Munari, U. 2000, in *Asymmetrical Planetary Nebulae II: From Origins to Microstructures*, ASP Conference Series, Vol. 199, ed. J. H. Kastner, N. Soker, & S. Rappaport (ASP: San Francisco), 199
- Dougherty, S. M. & Williams, P. M. 2000, *MNRAS*, 319, 1005
- Jura, M. & Helfand, D. J. 1984, *ApJ*, 287, 785
- Karovska, M., Hack, W., Raymond, J., & Guinan, E. 1997, *ApJ*, 482, L175
- Karovska, M., Nisenson, P., Papaliolios, C., & Boyle, R. P. 1991, *ApJ*, 374, L51
- Karovska, M., Schlegel, E., Hack, W., Raymond, J. C., & Wood, B. E. 2005, *ApJ*, 623, L137
- Kastner, J. H. & Soker, N. 2004, *ApJ*, 616, 1188
- Kenny, H. T. & Taylor, A. R. 2005, *ApJ*, 619, 537
- Munari, U. & Renzini, A. 1992, *ApJ*, 397, L87
- Osterbrock, D. E. 1989, *Astrophysics of Gaseous Nebulae and Active Galactic Nuclei* (University Science Books: Sausalito)
- Reid, M. J. & Goldston, J. E. 2002, *ApJ*, 568, 931
- Reid, M. J. & Menten, K. M. 1997, *ApJ*, 476, 327
- Reimers, D. & Cassatella, A. 1985, *ApJ*, 297, 275
- Seaquist, E. R., Taylor, A. R., & Button, S. 1984, *ApJ*, 284, 202

Taylor, A. R. & Seaquist, E. R. 1984, ApJ, 286, 263

Taylor, A. R. & Seaquist, E. R. 1990, ApJ, 349, 313

Whitelock, P. A. 1987, PASP, 99, 573

Wood, B. E., Karovska, M. & Raymond, J. C. 2002, ApJ, 575, 1057

Wood, B. E. and Karovska, M. 2004, ApJ, 601, 502

Wright, A. E. & Barlow, M. J. 1975, MNRAS, 170, 41

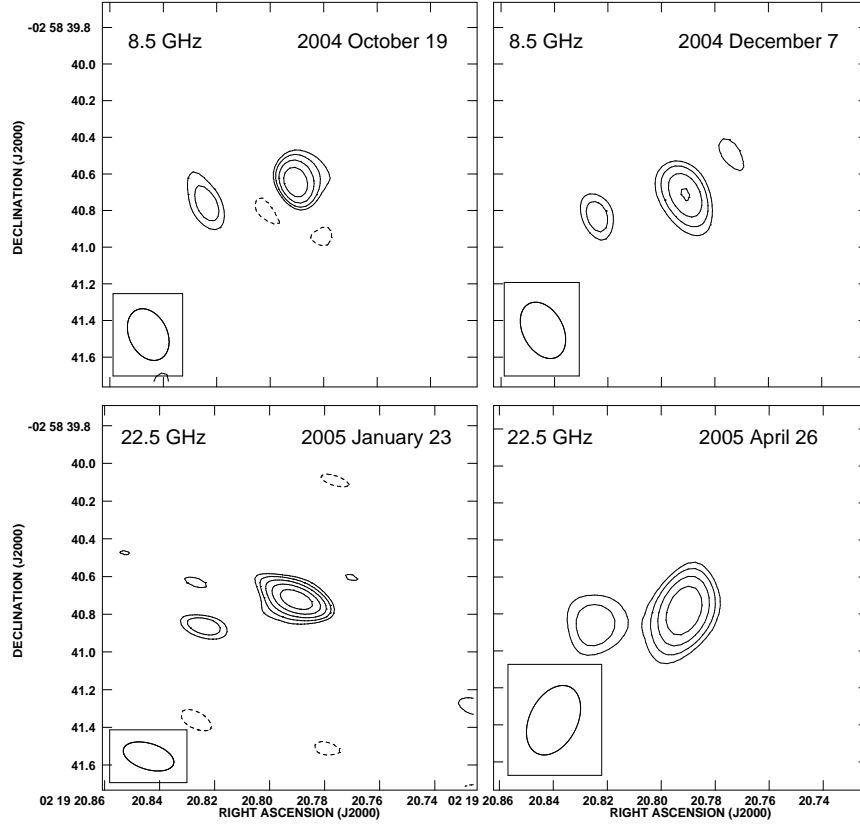


Fig. 1.— Radio continuum images of Mira AB obtained with the VLA at 8.5 GHz (top) and 22.5 GHz (bottom) on four different dates. Mira A is near the center of each panel, and Mira B is $\sim 0''.5$ to the southeast. Contour levels are $(-4.2, -3.0, 3.0, 4.2, 6, 8.5) \times 0.025$ mJy beam $^{-1}$ for the 8.5 GHz images and $(-4.2, -3.0, 3.0, 4.2, 6, 8.5, 12) \times 0.066$ mJy beam $^{-1}$ for the 22.5 GHz images. The lowest contour levels are $\sim 3\sigma$. The restoring beams are shown in the lower left corner of each panel. Both stars are consistent with point sources.

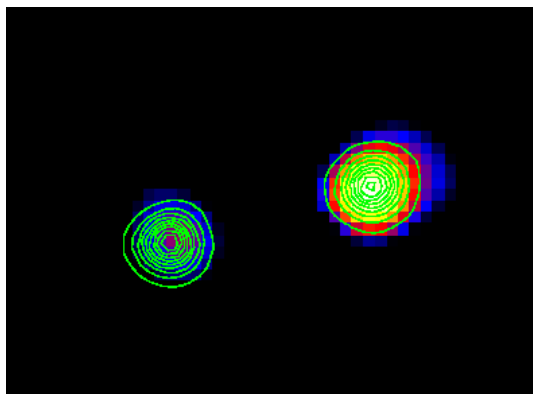


Fig. 2.— Contours of an *HST* 3729Å image of Mira AB from 2004 February (Karovska et al. 2005) overlaid on a VLA 8.5 GHz image of Mira AB from 2004 October. The VLA image was restored using a circular beam with FWHM $0''.25$. The *HST* contours show 10% brightness increments. For display purposes, the intensity peaks of Mira A have been aligned in the two images. The field-of-view is $\sim 1''.2 \times 0''.85$. North is on top, east to the left.

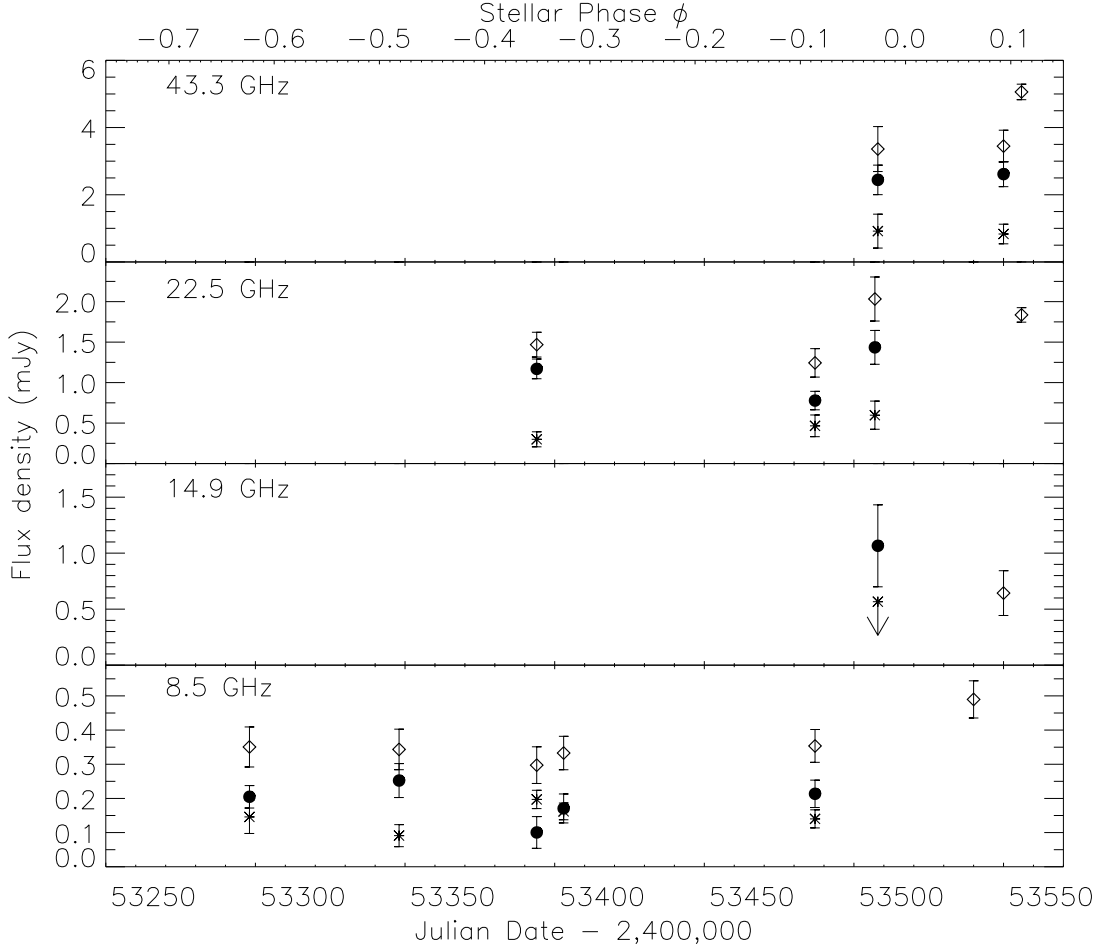


Fig. 3.— Plots of radio continuum flux density in mJy as a function of time for the two components of Mira AB at four frequencies. Values for Mira A are plotted as closed circles, and those for Mira B as asterisks. Diamonds represent the sum of the two components. In cases where A & B were unresolved, only the combined flux density is shown. The 1σ error bars indicate statistical uncertainties but do not include calibration uncertainties. The optical stellar phase of Mira A is shown along the upper axis; its optical maximum occurs at $\phi=0$, and optical minimum at $\phi = -0.36$. The individual 8.5 GHz flux densities for the two stellar components on JD 2,453,394 and 2,453,403 are unreliable (see Text).

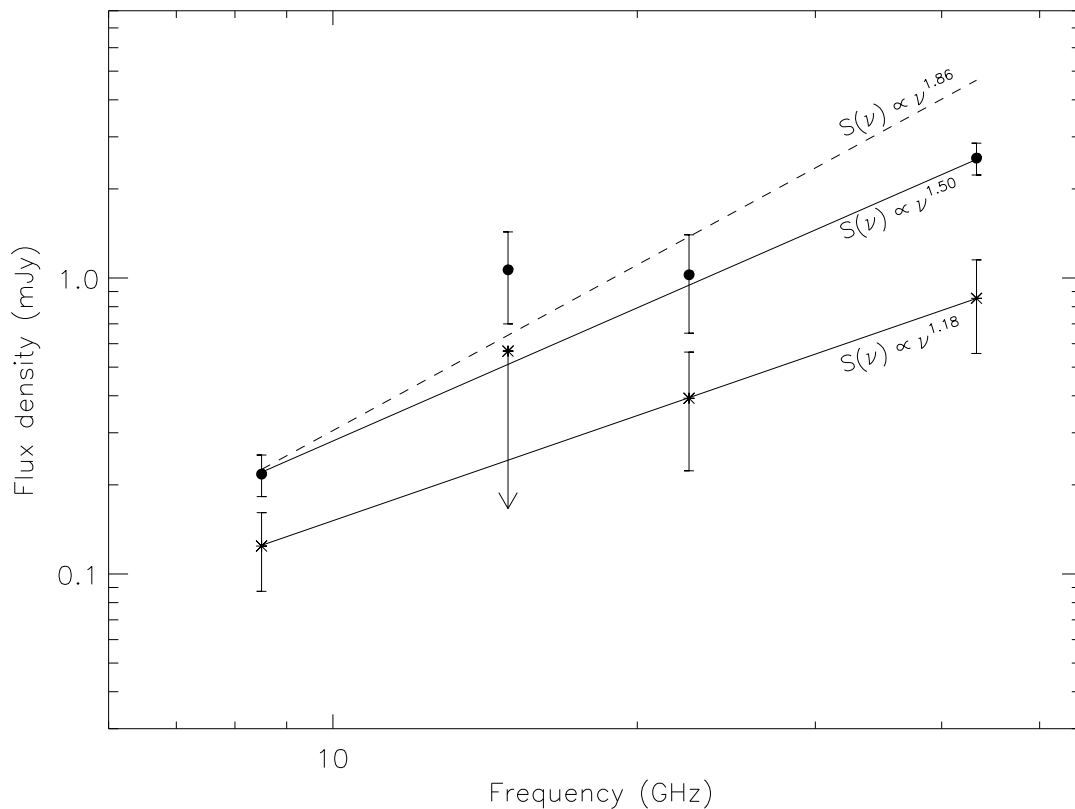


Fig. 4.— Radio frequency spectra for Mira A (closed circles) and Mira B (asterisks). Points at each frequency represent a weighted mean of all data from Table 1 for which the stellar components could be resolved sufficiently to permit individual flux density measurements. Error bars include both measurement scatter and systematic uncertainties. A 3σ upper limit is shown for Mira B at 14.9 GHz. Overplotted are the best-fitting power laws of the form $S(\nu) \propto \nu^\alpha$ (solid lines), as well as the predicted spectrum based on the static photosphere model of Reid & Menten 1997 (dashed line).

Table 1. VLA Monitoring Data for Mira A & B

Julian Date	Array Configuration	ν (GHz)	Image rms (mJy beam ⁻¹)	Flux Density A (mJy)	Flux Density B (mJy)	Flux Density A+B (mJy)	Flux Density ^a 0215-023 (Jy)	Resolved?
2,453,298	A	8.5	0.03	0.20±0.03	0.14±0.05	0.34±0.06	0.765±0.004	F
2,453,348	A	8.5	0.02	0.25±0.05	0.09±0.03	0.34±0.06	0.764±0.005	F
2,453,394	BnA	8.5	0.03	0.10±0.05 ^b	0.20±0.03 ^b	0.30±0.05	0.769±0.003	P
2,453,394	BnA	22.5	0.07	1.17±0.12	0.30±0.09	1.47±0.15	0.500±0.005	F
2,453,403	BnA	8.5	0.02	0.17±0.04 ^b	0.16±0.02 ^b	0.33±0.05	0.794±0.002	P
2,453,487	B	8.5	0.03	0.21±0.04	0.14±0.03	0.35±0.05	0.786±0.003	P
2,453,487	B	22.5	0.06	0.78±0.11	0.46±0.13	1.24±0.18	0.468±0.006	F
2,453,507	B	22.5	0.12	1.44±0.21	0.60±0.17	2.04±0.27	0.495±0.003	F
2,453,508	B	14.9	0.16	1.06±0.37	< 0.57 ^c	<1.63	0.652±0.002	F
2,453,508	B	43.3	0.26	2.44±0.44	0.92±0.50	3.36±0.67	0.284±0.006	F
2,453,540	CnB	8.5	0.03	0.49±0.05	0.800±0.001	U
2,453,550	CnB	14.9	0.14	0.64±0.20	0.651±0.001	U
2,453,550	CnB	43.3	0.19	2.61±0.37	0.83±0.29	3.44±0.47	0.265±0.004	F
2,453,556	CnB	22.5	0.05	1.84±0.09	0.485±0.004	U
2,453,556	CnB	43.3	0.13	5.06±0.23	0.265±0.003	P

Note. — Julian date (JD) 2,453,298 corresponds to 2004 October 19 and JD 2,453,556 to 2005 July 4. The last column indicates the degree of spatial resolution of Mira A & B: F=fully resolved, P=partially resolved, U=unresolved.

^aAmplitude and phase calibrator; the absolute flux scale was established using observations of 3C48 plus clean-component models of this source. Adopted fluxes for 3C48 were: 3.15 Jy (8 GHz); 1.74 Jy (15 GHz), 1.12 Jy (22 GHz), and 0.53 Jy (43 GHz). Calibration uncertainties are ~10% at 8 GHz, 15 GHz, & 22 GHz, and ~20% at 43 GHz.

^bFlux densities of individual components are unreliable (see Text).

^c3 σ upper limit.